Preferential Proton over Electron heating from coherent structures during the first perihelion of Parker Solar Probe.

Nikos Sioulas [ID],[1] Chen Shi(时辰) [ID],[2] Zesen Huang (黄泽森) [ID],[2] and Marco Velli [ID][1]

[1]*Earth, Planetary, and Space Sciences, University of California, Los Angeles*
Los Angeles, CA 90095, USA
[2]*Department of Earth, Planetary, and Space Sciences, University of California, Los Angeles*
Los Angeles, CA, USA

ABSTRACT

The solar wind undergoes significant heating as it propagates away from the Sun; the exact mechanisms responsible for this heating remain unclear. Using data from the first perihelion of the Parker Solar Probe mission, we examine the properties of proton and electron heating occurring within magnetic coherent structures identified by means of the Partial Variance of Increments (PVI) method. Statistically, regions of space with strong gradients in the magnetic field, $PVI \geq 1$, are associated with strongly enhanced proton but only slightly elevated electron temperatures. Our analysis indicates a heating mechanism in the nascent solar wind environment facilitated by a nonlinear turbulent cascade that preferentially heats protons over electrons.

Keywords: Parker Solar Probe, Electron Heating, Solar Wind, MHD Turbulence, Intermittency

1. INTRODUCTION

Within the inner heliosphere, the ion temperature of the solar wind decays as a function of radial distance as $T_p \sim r^{-\gamma_p}$, where, $0.5 \lesssim \gamma_p \lesssim 1$, (Richardson et al. 1995; Stansby et al. 2018), while, the electron temperature as $T_e \sim r^{-\gamma_e}$, where $0.3 \lesssim \gamma_e \lesssim 0.7$ (Maksimovic et al. 2005; Boldyrev et al. 2020). As a result, the electron and proton temperatures of the solar wind decay at much slower rates than predicted by spherically symmetric adiabatic expansion models (i.e. $T \sim r^{-4/3}$). In order to fully understand solar wind dynamics, supplementary heating processes must be considered (Matthaeus & Velli 2011). In recent years, a multitude of mechanisms for transferring turbulent energy into thermal degrees of freedom in weakly collisional plasmas have been explored, including, wave-particle interactions (Isenberg & Hollweg 1983; Leamon et al. 1999; Bourouaine et al. 2012; González et al. 2021), and, non-resonant mechanisms such as stochastic heating (Chandran et al. 2010; Bourouaine & Chandran 2013). Another potential source of non-adiabatic heating is the magnetohydrodynamic turbulence in the solar wind (Coleman 1968). In particular, observational and numerical studies indicate that plasma heating occurs in an intermittent fashion and suggest a statistical link between coherent magnetic field structures (CSs) and elevated temperatures (Osman et al. 2012; Chasapis et al. 2015; Yordanova et al. 2021; Sioulas et al. 2022a,b). The intermittent character of turbulence can

be attributed to a fractally distributed population of small-scale CSs, superposed on a background of random fluctuations that, despite occupying only a minor fraction of the entire dataset (Vlahos et al. 2008; Parashar et al. 2009; Osman et al. 2012; Wan et al. 2012; Sioulas et al. 2022a,b) can account for a disproportionate amount of magnetic energy dissipation, and heating of charged particles (Karimabadi et al. 2013; Sioulas et al. 2020a,b; Bandyopadhyay et al. 2020).

It is essential that the dominant heating mechanism(s) is/are consistent with a broad range of in situ, as well as remote observations, including (1) The heating must be spatially extended out to several solar radii in order to drive observed wind speed (2) The preferential heating of protons in the direction perpendicular to the magnetic field (3) The preferential heating of protons over electrons, with heavier ion heating being even more pronounced.

In this study, we aim to investigate the proton *vs.* electron heating in the nascent solar wind environment. For this reason, we analyze the Quasi-Thermal Noise (QTN) electron data and proton data from the Solar Probe Analyzer (SPAN) part of the Solar Wind Electron, Alpha, and Proton (SWEAP) suite (Kasper et al. 2016) during the first encounter of Parker Solar Probe mission (PSP) with the Sun (Fox et al. 2016). As a first step, we utilize the Partial Variance of Increments (PVI) method to identify the underlying coherent structures in our dataset and then use a superposed-epoch analysis to study the effects of CS's method on charged particle heating. We show that both ions and electrons are heated in the vicinity of CSs, however, the effect is considerably less efficient for electrons. The structure of this paper is as follows: Section 2, describes the Partial Variance of Increments methods, the diagnostic used in this study to identify coherent structures; Section 3 presents the selected data and their processing; In Section 4 we present the results of this study; Section 5 provides a summary of the results and conclusions.

2. BACKGROUND

Since the beginning of in situ observations, it has been revealed that several types of localized coherent structures abound in the solar wind (Tsurutani & Smith 1979; Hudson 1971). A number of recent studies suggest that CSs are dynamically generated as a by-product of the turbulent cascade (Matthaeus & Lamkin 1986; Veltri 1999; Sioulas et al. 2022), or/and are of coronal origin being passively advected by the solar wind (Borovsky 2021). The borders of such structures have been shown to remain in a dynamic state and have been associated with strong gradients in the turbulent fields resulting in local nonlinear interactions and processes such as magnetic reconnection or various types of instabilities (Matthaeus et al. 2015). The Partial variance of Increments method PVI, is an analytical tool for detecting sharp gradients in a turbulent field and can be estimated as (Greco et al. 2008)

$$PVI(t,\ell) = \frac{|\delta\boldsymbol{B}(t,\tau)|}{\sqrt{\langle|\delta\boldsymbol{B}(t,\tau)|^2\rangle}}, \qquad (1)$$

where, $|\Delta\mathbf{B}(t,\tau)| = |\mathbf{B}(t+\tau) - \mathbf{B}(t)|$ is the magnitude of the magnetic field vector increments, and $\langle...\rangle$ represents the average over a large window that is a multiple of the estimated magnetic field correlation time. As the PVI index increases, the identified events are more likely to be associated with Non-Gaussian structures that lay on the "heavy tails" observed in the PDF of scale-dependent increments, suggesting that coherent structures correspond to events of index $PVI \geq 2.5$. The most intense magnetic field discontinuities, such as current sheets and reconnection sites, can then be identified by further raising the threshold value to $PVI \geq 4$, and, $PVI \geq 6$, respectively (Servidio et al. 2009).
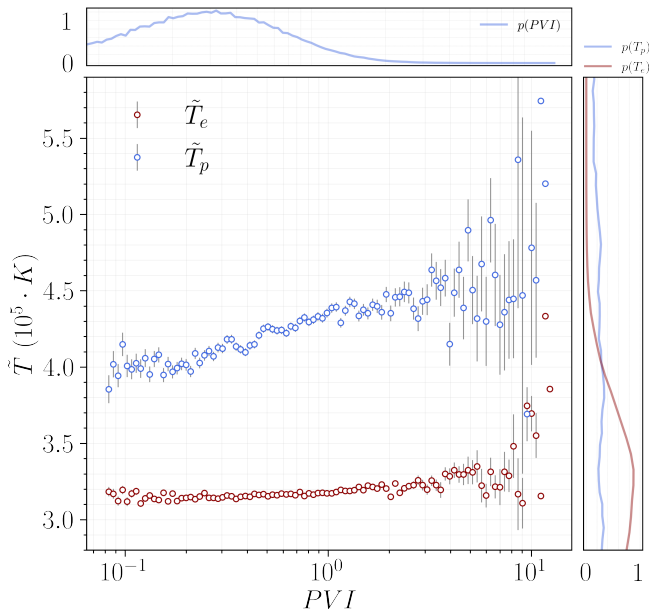
Figure 1. Binned mean of proton (T_p in blue) and electron temperature (T_e in red) plotted against PVI . Error bars are also shown indicating the standard error of the mean, $\sigma_i/\sqrt{n}$, where σ_i is the standard deviation of the samples inside the bin. The PDFs of the electron and proton temperature $p(T_e)$, $p(T_p)$ and the PVI index $p(PVI)$ are shown separately in red and blue on the top and right margin of the plot respectively.

3. DATA & ANALYSIS PROCEDURE

We have analyzed data from the first encounter E1 of PSP with the Sun, during the period November 1 - November 10, 2018. For magnetic field data, we use the SCaM data product, which merges fluxgate and search-coil magnetometer (SCM) measurements from the FIELDS instrument (Bale et al. 2016) by making use of frequency-dependent merging coefficients, thus enabling magnetic field observations from DC to 1MHz with an optimal signal-to-noise ratio (Bowen et al. 2020). Proton data were obtained from the Solar Wind Electron, Alpha, and Proton (SWEAP) suite (Kasper et al. 2016), and electron data derived from the Quasi-thermal noise from the FIELDS instrument (Moncuquet et al. 2020). Note, that the same electron analysis was repeated by tak-

ing into account core temperature data fitted from the SPAN-e electron VDFS (Halekas et al. 2020), with qualitatively similar results.

In order to estimate the PVI timeseries, SCaM magnetic field data have been linearly interpolated to a cadence of $\delta\tau = 0.05$s. Subsequently, following Equation 1, the PVI timeseries was estimated using an averaging window of duration $d = 8$ hours, which was several times the estimated correlation time of the magnetic field for E1 of PSP (Chhiber et al. 2020). Note that the analysis was also carried out for various averaging times (from 1 to 12 hours) and it was observed to have minimal impact on the final result. Finally, the PVI time series was resampled to the electron timeseries cadence of 7 seconds, and proton timeseries cadence of ~ 28 seconds in a way such that for each interval the mean value of PVI in that interval was chosen. Note, that the same analysis was repeated by choosing the maximum value of PVI within each interval with qualitatively similar results. Additionally, the lower resolution data for the proton timeseries do not affect the final conclusion of this work, as the results presented here are in agreement with (Sioulas et al. 2022b) who studied the correlation between PVI and proton temperature for the first six encounters of PSP using high resolution (0.873 seconds) proton data from the Solar Probe Cup Instrument (SPC) data (Kasper et al. 2016).

4. RESULTS

In this section, we investigate the contribution of coherent structures, identified by means of the PVI method (see Section 3), to the heating of protons and electrons in the solar wind. The first step in this analysis is to interpret T_p as a function of PVI through binned statistics. Figure 1 shows the average proton (blue) and electron (red) temperature per bin using 100 PVI bins (i.e., $\langle T_p(\theta_i \leq PVI \leq \theta_{i+1})\rangle$, where θ_i is the PVI threshold) plotted against the center of the bin. Uncertainty bars are also
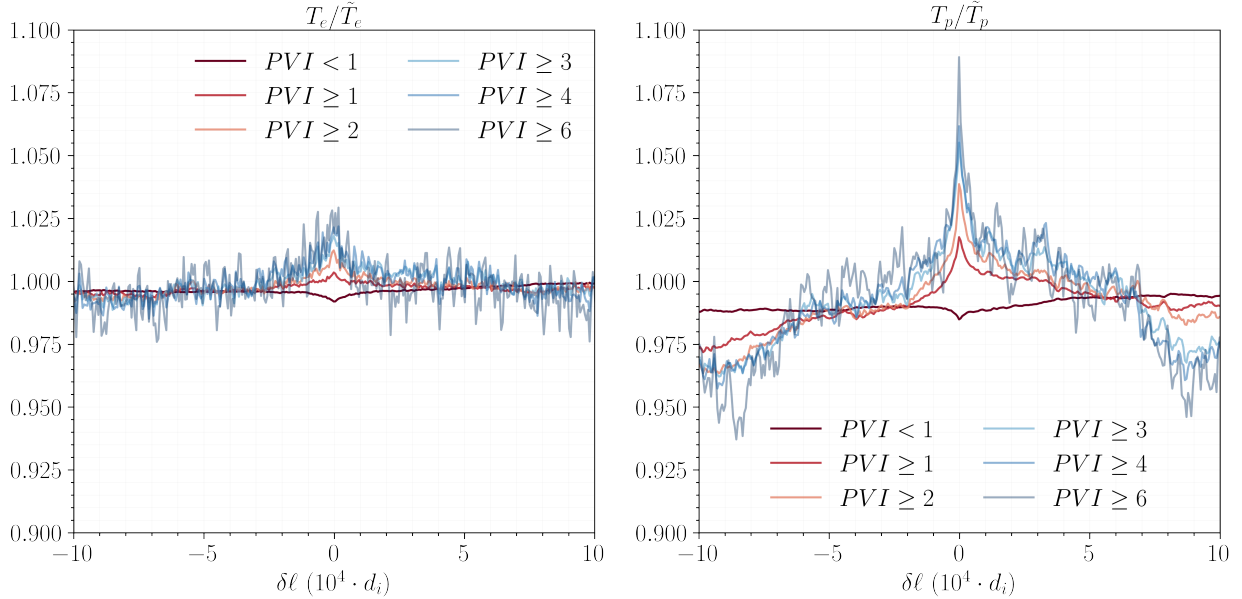
Figure 2. Average (a) T_e (b) T_p conditioned on the spatial lag, normalized to the ion inertial length d_i, estimate separation from PVI events that exceed a PVI threshold. Note that T_j, $j = e$, p has been normalized by the average value $\tilde{T}_j$ within a window that spans $\delta\ell = 2 \cdot 10^5 d_i$ and is centered around the discontinuity under study.

shown indicating the standard error of the sample (Gurland & Tripathi 1971). In this case, the uncertainty is estimated as $\sigma_i/\sqrt{n}$, where σ_i is the standard deviation of the samples inside the bin. The PDFs of the electron and proton temperature $p(T_e)$, $p(T_p)$, as well as, the PDF of the PVI index $p(PVI)$ are shown separately in blue and red on the top and right margin of the plot. In agreement with previous studies (Osman et al. 2012; Yordanova et al. 2021; Sioulas et al. 2022a) a statistically significant positive correlation is observed with high PVI index and elevated T_p. Nevertheless, the limited number of observations for $PVI \geq 4$ results in high variability of T_p on the right-hand side of the figure. More specifically, the lowest observed PVI values, $PVI \sim 10^{-1}$, are associated with a proton temperature of $T_p \sim 4 \cdot 10^5$ K, while for $PVI \sim 4$ the proton temperature raises to $T_p \sim 4.6 \cdot 10^5$ K. On the other hand, for electrons, only a moderate positive statistical correlation is observed. In particular coherent structures characterized by a PVI index, $PVI \leq 1$, hardly change the electron

temperature, while for higher PVI thresholds a rough statistical trend is observed. Note, that several bins with $PVI \sim 10$, usually associated with reconnection exhausts (Servidio et al. 2012), display considerably increased electron temperatures $T_e \geq 3.5 \cdot 10^5$ K. This could indicate that magnetic reconnection plays a major role in electron heating observed in the solar wind. However, further study is needed to identify these structures and determine whether magnetic reconnection is indeed responsible for the observed heating, and whether other mechanisms are involved.

To gain a deeper understanding of the relationship between the temperature of the solar wind, and magnetic field discontinuities, we estimate averages of T_j, where, $j = e$, p the temperature of electrons and protons respectively, constrained by the temporal separation between PVI events that belong to a given PVI bin.

This can be formally expressed as (Tessein et al. 2013; Sorriso-Valvo et al. 2018):

$$\langle T_j(\Delta t,\, \theta_i,\, \theta_{i+1})\rangle \;=\; \langle T_j(t_{PVI} + \Delta t)|PVI \geq \theta_i\rangle, \tag{2}$$

where, Δt is the temporal lag relative to the location of the main PVI event taking place at time t_{PVI}, and $\theta = [0, 1, 2, 3, 4, 6]$. Fig. 2 illustrates the conditional average of electron and proton temperature in the left and right panel respectively at different spatial lags. Note, that temporal lags have been converted to spatial lags, subject to the validity of Taylor's hypothesis (Taylor 1938), $\ell = V_{SW}\Delta t$. For a direct comparison between different plasma environments and to cast our results in physically relevant units, spatial scales have been normalized by the ion inertial length $d_i = V_A/\Omega_i$, where $\Omega_i = \frac{eB}{m_p}$, is the proton gyrofrequency, e is the elementary charge, B is the mean magnetic field, and m_p is the mass of the proton (Schekochihin et al. 2009). Additionally, for each identified event the temperature T_j was normalized by the average value $\tilde{T}_j$ within a window that spans $\delta\ell = 2\cdot 10^5 d_i$ and is centered around the discontinuity under study. This allows us to disentangle our observations from the effects of transients such as Heliospheric Current Sheet (HCS) crossings, usually associated with minima in solar wind temperature (Suess et al. 2009; Shi et al. 2022), Switchback patches, observed to enhance the solar wind temperature (Shi et al. 2022) etc. Additionally, it enables us to get a more direct estimate of the relative contribution of CSs to the internal energy of the charged particle species under investigation.

It appears that no significant proton and electron heating of the solar wind occurs at times when the magnetic field is relatively smooth, as indicated by the dip in the normalized mean temperature at lag equal to $t = 0$s for $PVI \leq 1$. Increasing the threshold value θ, however, results in a global maximum in normalized T_j

close to zero lag, suggesting that both proton and electron temperatures will rise in the vicinity of coherent structures. It can be readily seen, however, that the heating process is less pronounced in the case of the electrons, since, T_e does not considerably deviate from the mean $\tilde{T}_e$. On the other hand, proton temperature considerably increases near CSs as illustrated in Figure 2b, with the enhancement being progressively more obvious as we consider higher PVI thresholds. There is a distinct rate of decrease for each bin, with the steepest gradients in T_p observed around the sharpest discontinuities, $PVI \geq 6$. T_p remains elevated near the main event, most likely because of the clustering of coherent structures (Yordanova et al. 2021; Sioulas et al. 2022b).

5. SUMMARY AND CONCLUSIONS

Using observations from PSP's first encounter with the Sun, we investigated the relationship between the proton and electron heating with coherent magnetic structures in the young solar wind environment. Seeking to better understand turbulent dissipation in the vicinity of solar wind sources we have first identified coherent structures in our dataset using the PVI method (Greco et al. 2008). Subsequently, the effect of CSs on the heating of electrons and protons was examined. The electron temperature here is obtained from QTN-spectroscopy (Moncuquet et al. 2020), which indicates the temperature of the distribution's core.

Our preliminary analysis corroborates previous results (Osman et al. 2012; Sorriso-Valvo et al. 2019; Qudsi et al. 2020; Yordanova et al. 2021; Sioulas et al. 2022b) and indicates that coherent structures can provide a channel for ion heating in the young solar wind. However, enhancements in electron temperature are considerably less significant and it would be challenging to imagine that intermittent heating could account for the non-adiabatic cooling profile of electrons in the solar wind. One possible expla-

nation for the preferential intermittent heating of protons over electrons is the "helicity barrier" mechanism that prevents turbulence energy cascade to electron scales so it can effectively heat the electrons (Squire et al. 2022). In the case where the system is continuously driven, the large-scale energy will grow in time as the parallel correlation length decreases (Meyrand et al. 2021). It is through this growth that turbulent energy is eventually funneled into a spectrum of high-frequency ion-cyclotron waves (ICWs), which end up primarily heating the ions.

As a result of our study, we gained a better understanding of how turbulent dissipation and heating of electrons and protons occur in the near Sun solar wind environment. The main finding of this study is that proton heating from coherent structures in the nascent solar wind is preferential to electron heating. However, our results present only a preliminary comparison of electron and proton heating in the near sun solar wind. A complete understanding of how particle heating and dissipation occur at iner-

tial and kinetic scales, will require a more thorough statistical analysis considering a larger and higher resolution dataset. Additionally, strahl, and halo components of the electron distribution function will need to be studied to provide a more complete understanding on how different electron populations behave in the vicinity of CSs.

Our results will guide future works that model the heating of the solar corona and the nascent solar wind environment.

REFERENCES

Bale, S. D., Goetz, K., Harvey, P. R., et al. 2016, r, 204, 49, doi: 10.1007/s11214-016-0244-5

Bandyopadhyay, R., Matthaeus, W. H., Parashar, T. N., et al. 2020, The Astrophysical Journal Supplement Series, 246, 61, doi: 10.3847/1538-4365/ab6220

Boldyrev, S., Forest, C., & Egedal, J. 2020, Proceedings of the National Academy of Science, 117, 9232, doi: 10.1073/pnas.1917905117

Borovsky, J. E. 2021, Frontiers in Astronomy and Space Sciences, 8, doi: 10.3389/fspas.2021.721350

Bourouaine, S., Alexandrova, O., Marsch, E., & Maksimovic, M. 2012, ApJ, 749, 102, doi: 10.1088/0004-637X/749/2/102

Bourouaine, S., & Chandran, B. D. G. 2013, ApJ, 774, 96, doi: 10.1088/0004-637X/774/2/96

Bowen, T. A., Bale, S. D., Bonnell, J. W., et al. 2020, Journal of Geophysical Research: Space Physics, 125, e2020JA027813, doi: https://doi.org/10.1029/2020JA027813

Chandran, B. D. G., Li, B., Rogers, B. N., Quataert, E., & Germaschewski, K. 2010, ApJ, 720, 503, doi: 10.1088/0004-637X/720/1/503

Chasapis, A., Retinò, A., Sahraoui, F., et al. 2015, ApJL, 804, L1, doi: 10.1088/2041-8205/804/1/L1

Chhiber, R., Goldstein, M. L., Maruca, B. A., et al. 2020, The Astrophysical Journal Supplement Series, 246, 31, doi: 10.3847/1538-4365/ab53d2

Coleman, Paul J., J. 1968, \apj, 153, 371, doi: 10.1086/149674

Fox, N. J., Velli, M. C., Bale, S. D., et al. 2016, r, 204, 7, doi: 10.1007/s11214-015-0211-6

Gonz á lez, C. A., Tenerani, A., Matteini, L., Hellinger, P., & Velli, M. 2021, The Astrophysical Journal Letters, 914, L36, doi: 10.3847/2041-8213/ac097b

Greco, A., Chuychai, P., Matthaeus, W. H., Servidio, S., & Dmitruk, P. 2008, Geophysical Research Letters, 35, doi: https://doi.org/10.1029/2008GL035454

Gurland, J., & Tripathi, R. C. 1971, The American Statistician, 25, 30. http://www.jstor.org/stable/2682923

Halekas, J. S., Whittlesey, P., Larson, D. E., et al. 2020, The Astrophysical Journal Supplement Series, 246, 22, doi: 10.3847/1538-4365/ab4cec

Hudson, P. 1971, Planetary and Space Science, 19, 1693, doi: https://doi.org/10.1016/0032-0633(71)90129-2

Isenberg, P. A., & Hollweg, J. V. 1983, J. Geophys. Res., 88, 3923, doi: 10.1029/JA088iA05p03923

Karimabadi, H., Roytershteyn, V., Wan, M., et al. 2013, Physics of Plasmas, 20, 012303, doi: 10.1063/1.4773205

Kasper, J. C., Abiad, R., Austin, G., et al. 2016, r, 204, 131, doi: 10.1007/s11214-015-0206-3

Leamon, R. J., Smith, C. W., Ness, N. F., & Wong, H. K. 1999, J. Geophys. Res., 104, 22331, doi: 10.1029/1999JA900158

Maksimovic, M., Zouganelis, I., Chaufray, J. Y., et al. 2005, Journal of Geophysical Research (Space Physics), 110, A09104, doi: 10.1029/2005JA011119

Matthaeus, W. H., & Lamkin, S. L. 1986, Physics of Fluids, 29, 2513, doi: 10.1063/1.866004

Matthaeus, W. H., & Velli, M. 2011, Space Science Reviews, 160, 145, doi: 10.1007/s11214-011-9793-9

Matthaeus, W. H., Wan, M., Servidio, S., et al. 2015, Philosophical Transactions of the Royal Society of London Series A, 373, 20140154, doi: 10.1098/rsta.2014.0154

Meyrand, R., Squire, J., Schekochihin, A. A., & Dorland, W. 2021, Journal of Plasma Physics, 87, doi: 10.1017/s0022377821000489

Moncuquet, M., Meyer-Vernet, N., Issautier, K., et al. 2020, The Astrophysical Journal Supplement Series, 246, 44, doi: 10.3847/1538-4365/ab5a84

Osman, K. T., Matthaeus, W. H., Wan, M., & Rappazzo, A. F. 2012, Phys. Rev. Lett., 108, 261102, doi: 10.1103/PhysRevLett.108.261102

Parashar, T. N., Shay, M. A., Cassak, P. A., & Matthaeus, W. H. 2009, Physics of Plasmas, 16, 032310, doi: 10.1063/1.3094062

Qudsi, R. A., Maruca, B. A., Matthaeus, W. H., et al. 2020, \apjs, 246, 46, doi: 10.3847/1538-4365/ab5c19

Richardson, J. D., Paularena, K. I., Lazarus, A. J., & Belcher, J. W. 1995, Geophysical Research Letters, 22, 325, doi: https://doi.org/10.1029/94GL03273

Schekochihin, A. A., Cowley, S. C., Dorland, W., et al. 2009, \apjs, 182, 310, doi: 10.1088/0067-0049/182/1/310

Servidio, S., Matthaeus, W. H., Shay, M. A., Cassak, P. A., & Dmitruk, P. 2009, Physical Review Letters, 102, 115003, doi: 10.1103/PhysRevLett.102.115003

Servidio, S., Valentini, F., Califano, F., & Veltri, P. 2012, \prl, 108, 045001, doi: 10.1103/PhysRevLett.108.045001

Shi, C., Velli, M., Tenerani, A., R é ville, V., & Rappazzo, F. 2022, arXiv:2201.02894 [astro-ph, physics:physics]. http://arxiv.org/abs/2201.02894

Shi, C., Panasenco, O., Velli, M., et al. 2022, arXiv e-prints, arXiv:2206.03807. https://arxiv.org/abs/2206.03807

Sioulas, N., Isliker, H., & Vlahos, L. 2020a, \apjl, 895, L14, doi: 10.3847/2041-8213/ab9092

—. 2022a, p, 657, A8, doi: 10.1051/0004-6361/202141361

Sioulas, N., Isliker, H., Vlahos, L., Koumtzis, A., & Pisokas, T. 2020b, \mnras, 491, 3860, doi: 10.1093/mnras/stz3259

Sioulas, N., Velli, M., Chhiber, R., et al. 2022b, Statistical analysis of intermittency and its association with proton heating in the near Sun environment

Sioulas, N., Huang, Z., Velli, M., et al. 2022, arXiv e-prints, arXiv:2206.00871. https://arxiv.org/abs/2206.00871

Sorriso-Valvo, L., Carbone, F., Perri, S., et al. 2018, Solar Physics, 293, doi: 10.1007/s11207-017-1229-6

Sorriso-Valvo, L., De Vita, G., Fraternale, F., et al. 2019, Frontiers in Physics, 7, doi: 10.3389/fphy.2019.00108

Squire, J., Meyrand, R., Kunz, M. W., et al. 2022, Nature Astronomy, doi: 10.1038/s41550-022-01624-z

Stansby, D., Salem, C., Matteini, L., & Horbury, T. 2018, SoPh, 293, 155, doi: 10.1007/s11207-018-1377-3

Suess, S. T., Ko, Y. K., von Steiger, R., & Moore, R. L. 2009, Journal of Geophysical Research (Space Physics), 114, A04103, doi: 10.1029/2008JA013704

Taylor, G. I. 1938, Proceedings of the Royal Society of London Series A, 164, 476, doi: 10.1098/rspa.1938.0032

Tessein, J. A., Matthaeus, W. H., Wan, M., et al. 2013, The Astrophysical Journal, 776, L8, doi: 10.1088/2041-8205/776/1/l8

Tsurutani, B. T., & Smith, E. J. 1979, Journal of Geophysical Research: Space Physics, 84, 2773, doi: https://doi.org/10.1029/JA084iA06p02773

Veltri, P. 1999, Plasma Physics and Controlled Fusion, 41, A787, doi: 10.1088/0741-3335/41/3a/071

Vlahos, L., Isliker, H., Kominis, Y., & Hizanidis, K. 2008, arXiv e-prints, arXiv:0805.0419. https://arxiv.org/abs/0805.0419

Wan, M., Matthaeus, W. H., Karimabadi, H., et al. 2012, PhRvL, 109, 195001, doi: 10.1103/PhysRevLett.109.195001

Yordanova, E., Vörös, Z., Sorriso-Valvo, L., Dimmock, A. P., & Kilpua, E. 2021, ApJ, 921, 65, doi: 10.3847/1538-4357/ac1942